

# Seismic scattering and absorption of oceanic lithospheric S waves in the Eastern North Atlantic



UNIVERSITÄT  
LEIPZIG



FRIEDRICH-SCHILLER-  
UNIVERSITÄT  
JENA



Katrin Hannemann<sup>1</sup>, Tom Eulenfeld<sup>2</sup>, Frank Krüger<sup>3</sup>, Torsten Dahm<sup>3,4</sup> (katrin.hannemann@uni-leipzig.de)

<sup>1</sup>Institute of Geophysics and Geology, Leipzig University; <sup>2</sup>Institute of Geosciences, Friedrich Schiller University Jena; <sup>3</sup>Institute of Geosciences, University of Potsdam; <sup>4</sup>Section 2.1: Physics of Earthquakes and Volcanoes, GFZ Potsdam

## Regional seismicity and Po/So waves

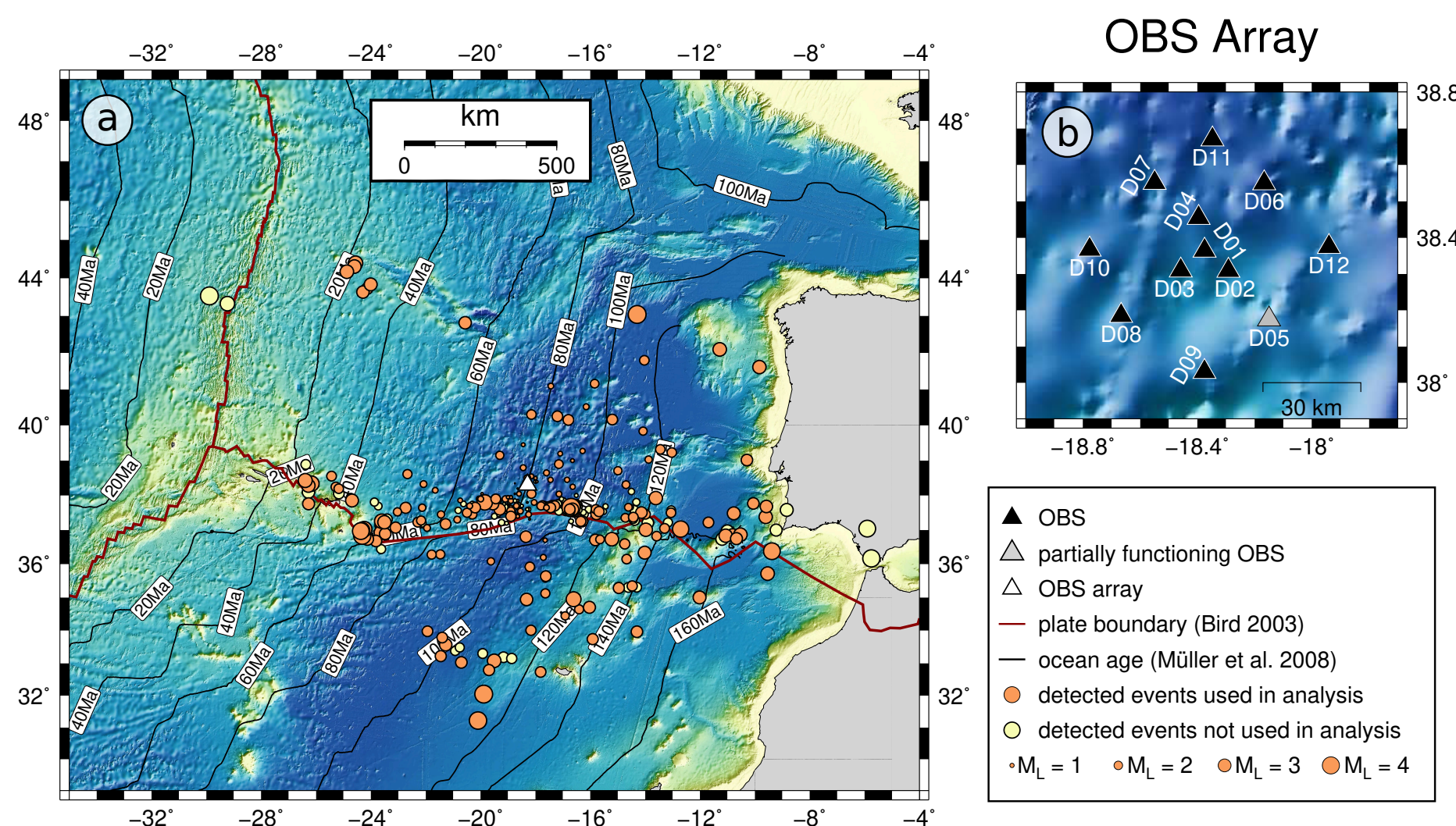


**Figure 1:** (a) Bathymetric map of the Eastern North Atlantic showing the distribution of earthquakes (light yellow and orange circles) detected by the OBS array (white triangle). Only events shown as orange circles were used in the analysis. Furthermore, the lithospheric ages are shown as contours. (b) Layout of the OBS array. The station shown in grey had clamped components and was therefore not used in the analysis.

We use a seismological array which was installed from July 2011 until April 2012 in 5000 m water depth about 100 km North of the Gloria fault. This fault defines the plate boundary between the Eurasian and African plate at this location (Fig. 1). The used array consists of 11 ocean bottom stations (OBS, Fig. 1 b). Within a 10 months period, we identified more than 350 local and regional earthquakes for epicentral distances up to 900 km (Fig. 1a) [Krüger et al., 2020].

The acquired earthquake recordings show high frequency (up to 30 Hz) P and S wave arrivals with tens of to hundred of seconds long seismic coda (Fig. 2). The waves travel with velocities indicating upper mantle material and are therefore referred to as oceanic Pn and Sn (Po and So) waves. They can be observed for events in up to 1000 km epicentral distances. Modelling results [Kennett and Furumura, 2013] suggest that these long high frequent codas originate from scattering in the oceanic mantle lithosphere.

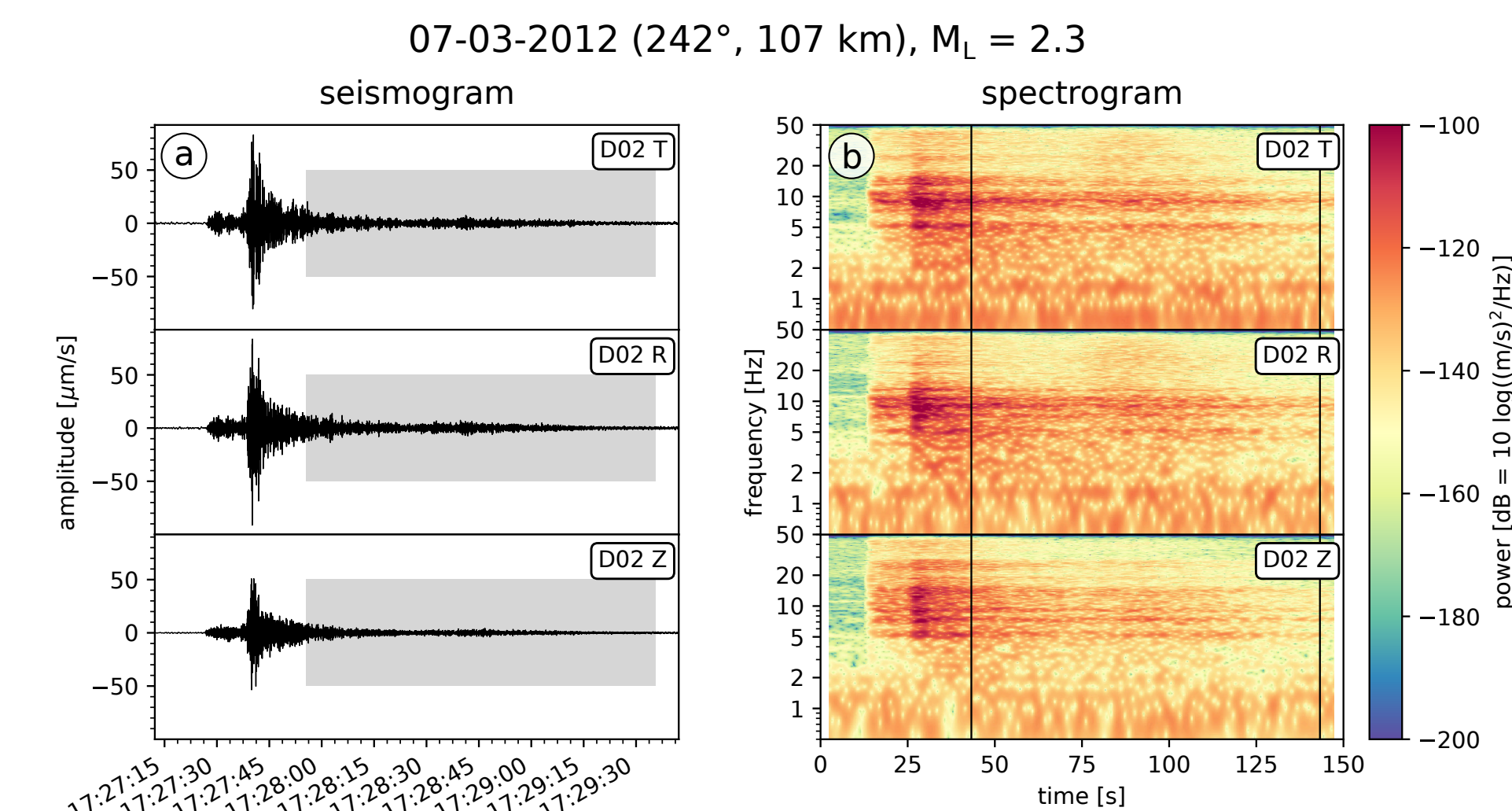


**Figure 2:** (a) Example for three component seismogram showing a regional event with characteristic Po and So waves. The data were high pass filtered at 0.88 Hz. The grey shaded areas mark the used coda wave time window. (b) Spectrograms for all three components of same event as presented in (a). The lines mark the used coda wave time window.

## Estimation of absorption and scattering

We use  $Q_{open}$  [Eulenfeld and Wegler, 2016] to determine intrinsic and scattering attenuation parameters of the recorded So wave energy by envelope inversion. Simulations [Kennett and Furumura, 2013] showed that So waves travel mainly in the oceanic lithosphere. Therefore, we use the analytical approximation for 2D isotropic radiative transfer [Paasschens, 1997] to model the recorded energy.

$$E_{mod}(t, r) = WR(r)G(t, r, g_0)e^{-bt}$$

$$G(t, r, g_0) = e^{-v_s t g_0} \frac{\delta(r - v_s t)}{2\pi v_s t} + \frac{g_0}{2\pi v_s t} \frac{1}{\sqrt{1 - \frac{r^2}{v_s^2 t^2}}} e^{g_0(\sqrt{v_s^2 t^2 - r^2} - v_s t)} \Theta(v_s t - r)$$

direct wave  
scattered wave

$g_0$  — (transport) scattering coefficient  
 $v_s$  — S wave velocity  
 $b$  — intrinsic attenuation coefficient  
 $R$  — energy site amplification factor  
 $r$  — source-receiver distance  
 $W$  — spectral source energy

We use the energy of all three seismometer components (Fig. 3) and a typical mantle S wave velocity of 4600 m/s for the inversion. The length of the used coda wave time window is based on the signal-to-noise ratio and shortened if additional energy arrives.

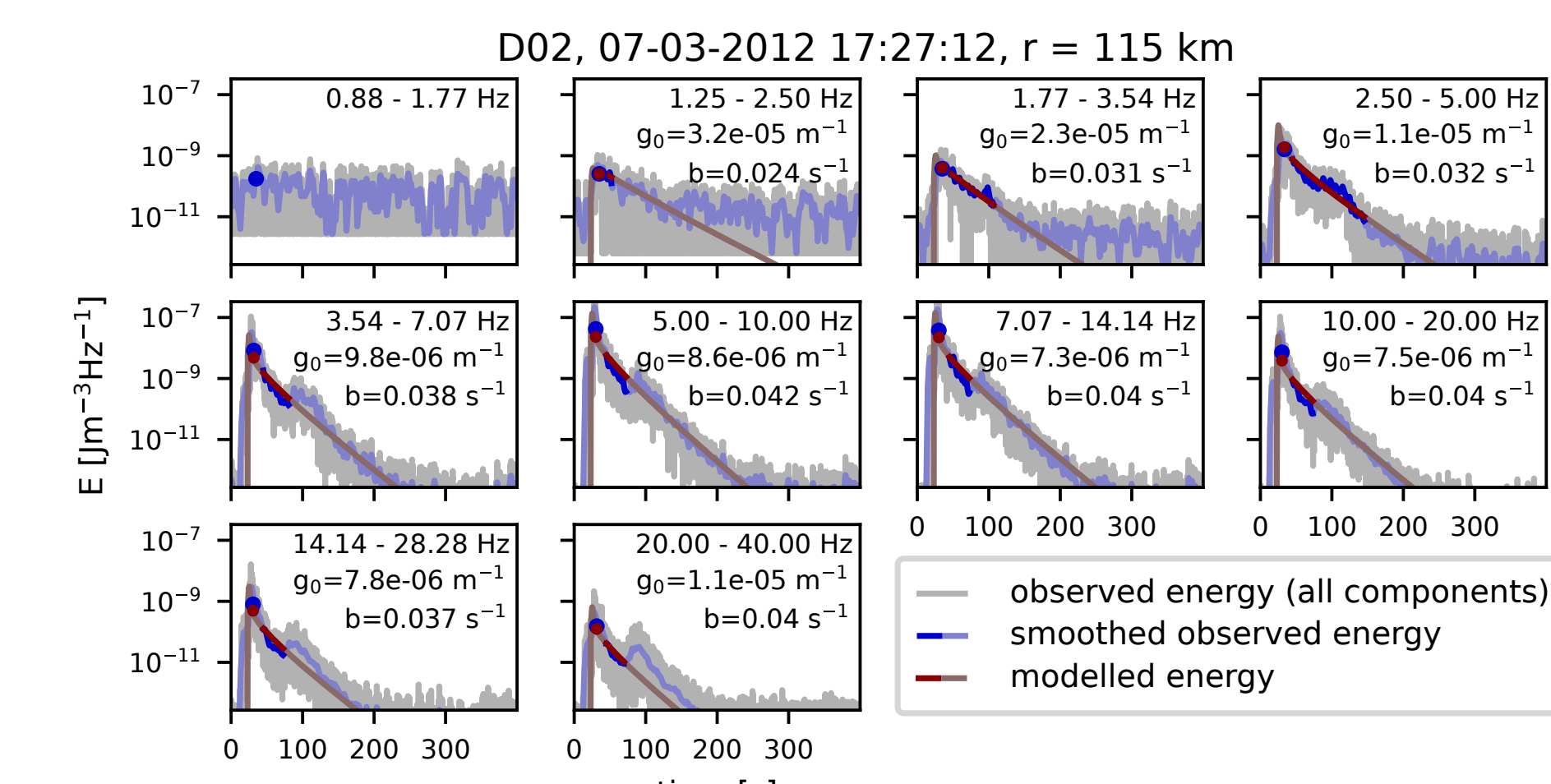


**Figure 3:** Comparison between observed and modelled energy densities at station D02 for event shown in Fig. 2 in all frequency bands used in the analysis. The used coda wave time windows are presented in darker colours.

## Results

We analyse the earthquake recordings in 45° azimuthal bins every 15° in order to compare the estimated attenuation parameters for different lithospheric ages. Some azimuthal bins had more events than others in the original catalog, we therefore divided each azimuthal bin in additional distance bins with a width of 50 km and selected the two to three largest events in each distance bin to get a similar number for each azimuth-distance bin (Fig. 4). The pre-selected events were inverted simultaneously for each azimuthal bin for a stable estimate.

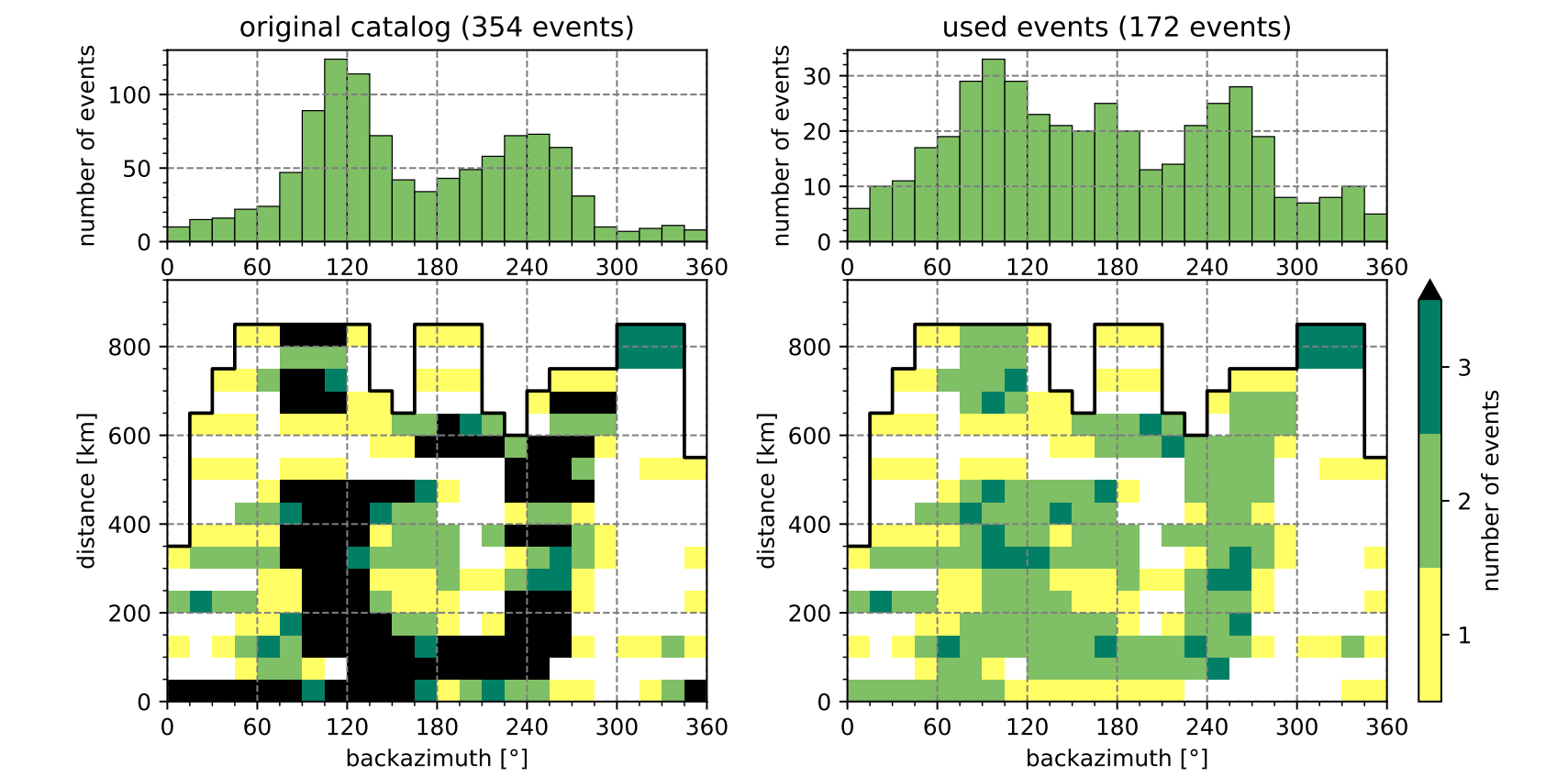


**Figure 4:** Azimuth-distance distribution of events.

We calculated inverse quality factors ( $Q^{-1}$ ) from the attenuation coefficients ( $g_0, b$ ).

$$Q_i^{-1} = \frac{b}{2\pi f}$$

$$Q_{sc}^{-1} = \frac{g_0 v_s}{2\pi f}$$

Furthermore, recordings with to short coda time windows (<5 s) were removed during the inversion. We therefore grouped the presented results based on the number of finally used events (indicated by transparency in Fig. 5).

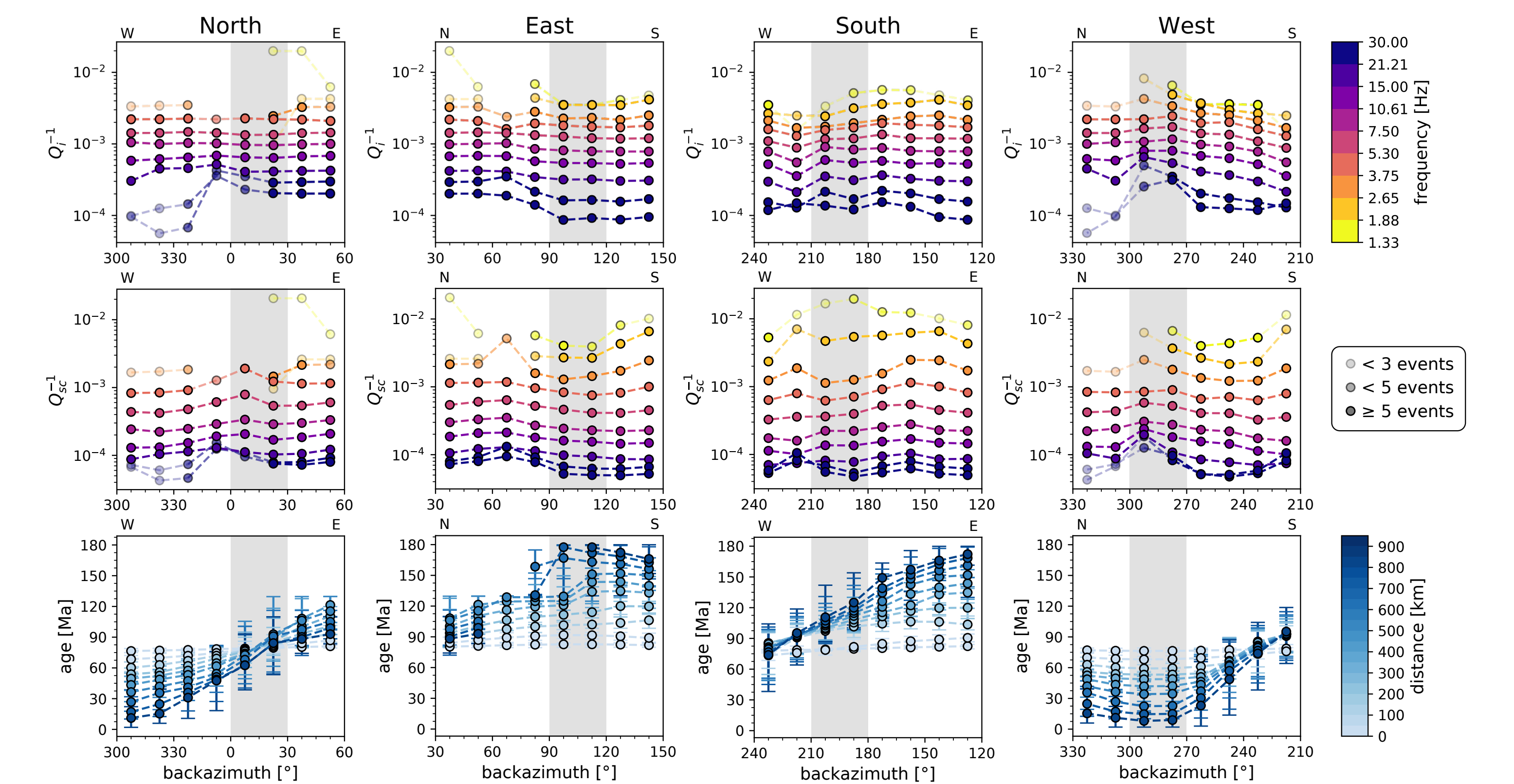


**Figure 5:** Estimated inverse quality factors for intrinsic ( $Q_i$ ) and scattering ( $Q_{sc}$ ) attenuation for different frequencies in each azimuthal bin and extracted median age and age range for each azimuth-distance bin [Müller et al., 2008]. Grey shaded areas mark data presented in Fig. 6. Transparency indicates number of used events. Note that the backazimuth axis of the Southern and Western azimuths are flipped.

## Conclusion

- scattering attenuation coefficients ( $g_0$ ):  $1 \cdot 10^{-6} - 4 \cdot 10^{-5} \text{ m}^{-1} \rightarrow$  typical for lithosphere or upper mantle [Sato et al., 2012]
- absorption and scattering attenuation: > 5 Hz increase in attenuation for decreasing lithospheric age (Fig. 6 a, b, c), in line with observation made by [Kennett et al., 2014]
- seismic albedo ( $B_0$ ): > 3 Hz scattering attenuation dominates or equal to intrinsic attenuation, for southern azimuths (green) scattering attenuation dominates for < 3 Hz  $\rightarrow$  probably influence of plate boundary (Fig. 6 e)
- absorption and mean free path length: 30–600 km (Fig. 6 f, g)  $\rightarrow$  weak influence of oceanic crust on So wave and its coda [Sato et al., 2012]

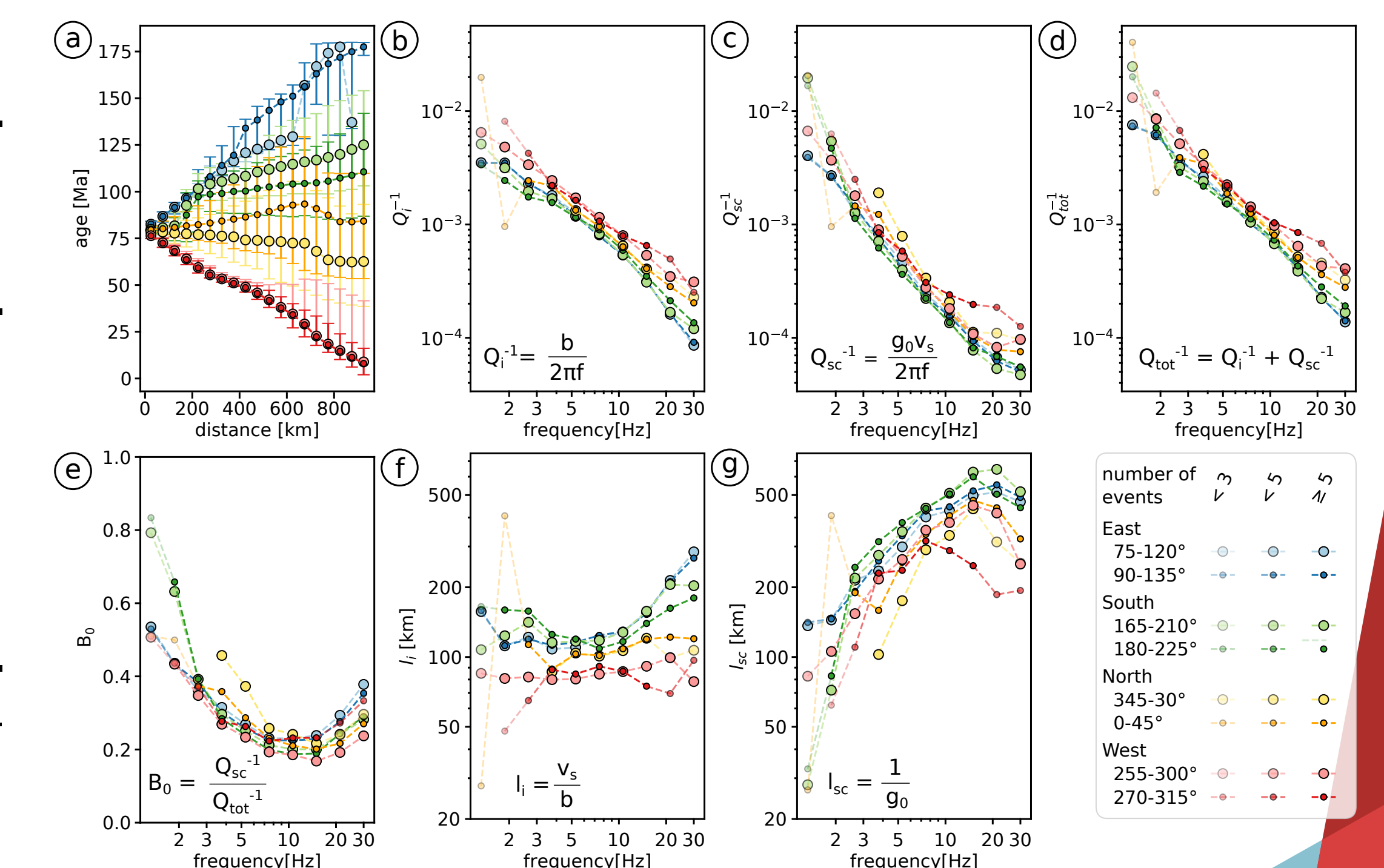


**Figure 6:** Comparison for (a) age-distance profiles, inverse Quality factors for (b) intrinsic attenuation, (c) scattering attenuation (d) total attenuation, (e) seismic albedo, (f) absorption path length and (g) mean free path for So waves for two profiles in each direction (East (blue), South (green), North (yellow/orange) and West (red)). The equations given in (b)–(g) illustrate how the corresponding values are calculated.  $v_s$  is the mantle S wave velocity (4600 m/s) with which the So waves travel.

Bird, (2003). An updated digital model of plate boundaries, *G3*, 4(3).  
 Eulenfeld and Wegler, (2016). Measurement of intrinsic and scattering attenuation of shear waves in two sedimentary basins and comparison to crystalline sites in Germany, *GJI*, 205(2): 744–757.  
 Kennett and Furumura, (2013). High-frequency Po/So guided waves in the oceanic lithosphere: I—long-distance propagation, *GJI*, 195(3): 1862–1877.  
 Kennett, B. L. N. et al., (2014). High-frequency Po/So guided waves in the oceanic lithosphere: II—heterogeneity and attenuation, *GJI*, 199(1): 614–630.  
 Krüger et al., (2020). Mapping of Eastern North Atlantic Ocean seismicity from Po/So observations at a mid-aperture seismological broad-band deep sea array, *GJI*, 221(2): 1055–1080.  
 Müller et al., (2008). Age, spreading rates and spreading symmetry of the world's ocean crust, *G3*, 9, Q04006.  
 Paasschens (1997). Solution of the time-dependent Boltzmann equation, *Phys. Rev. E* 56 1, 1135–1141.  
 Sato et al., (2012). Seismic Wave Propagation and Scattering in the Heterogeneous Earth, 2nd edn, Springer.